FULL PAPER

An Easily Sintered, Chemically Stable, Barium Zirconate-Based Proton Conductor for High-Performance Proton-Conducting Solid Oxide Fuel Cells

Wenping Sun,* Zhen Shi, Mingfei Liu, Lei Bi, and Wei Liu*

Yttrium and indium co-doped barium zirconate is investigated to develop a chemically stable and sintering active proton conductor for solid oxide fuel cells (SOFCs). $BaZr_{0.8}Y_{0.2-x}In_xO_{3-\delta}$ possesses a pure cubic perovskite structure. The sintering activity of $BaZr_{0.8}Y_{0.2-x}In_xO_{3-\delta}$ increases significantly with In concentration. $BaZr_{0.8}Y_{0.15}In_{0.05}O_{3-\delta}$ (BZYI5) exhibits the highest total electrical conductivity among the sintered oxides. BZYI5 also retains high chemical stability against CO_2, vapor, and reduction of H_2. The good sintering activity, high conductivity, and chemical stability of BZYI5 facilitate the fabrication of durable SOFCs based on a highly conductive BZYI5 electrolyte film by cost-effective ceramic processes. Fully dense BZYI5 electrolyte film is successfully prepared on the anode substrate by a facile drop-coating technique followed by co-firing at 1400 °C for 5 h in air. The BZYI5 film exhibits one of the highest conductivity among the $BaZrO_3$-based electrolyte films with various sintering aids. BZYI5-based single cells output very encouraging and by far the highest peak power density for $BaZrO_3$-based proton-conducting SOFCs, reaching as high as 379 mW cm^{-2} at 700 °C. The results demonstrate that Y and In co-doping is an effective strategy for exploring sintering active and chemically stable $BaZrO_3$-based proton conductors for high performance proton-conducting SOFCs.

1. Introduction

Solid oxide fuel cells (SOFCs) with high-temperature proton conductors (HTPCs) as electrolytes, which are usually called proton-conducting SOFCs, are considered to be the most promising next generation SOFCs working at intermediate/low-temperatures.[1–4] As is well known, electrolyte materials with high ionic conductivity are crucial for lowering the operating temperature of SOFCs, many attempts were tried to explore highly conductive ionic conductors in the past decades.[5,6] The activation energy for proton conduction is much lower than that for oxide ion conductors, and hence HTPCs have a great advantage of possessing high proton conductivity at reduced temperatures. HTPCs have attracted ever-growing interest since Iwahara et al. found proton conduction in some perovskite-type oxides under water-containing atmospheres at high temperatures.[4,7–11] HTPCs are also widely used in many other kinds of electrochemical devices, such as hydrogen separation membranes[12–17] and steam electrolysers.[18,19]

Due to the high conductivity and good sintering activity, acceptor-doped $BaCeO_3$ oxides have been widely used as electrolytes for SOFCs, and significant progress on optimization of electrolytes, electrode materials and fabrication techniques were achieved.[1,4,20–30] However, under CO_2 or water vapor-containing atmospheres, $BaCeO_3$-based oxides exhibit poor chemical stability,[2,21,31–36] which precludes their use in practical applications since water vapor is present in the electrode/electrolyte interface during fuel cell operation and the cathode side is exposed in CO_2-containing air. In contrast, acceptor-doped $BaZrO_3$ shows excellent chemical stability.[2,33,35–38] From the stability point of view, $BaZrO_3$-based oxides are the most promising electrolytes for proton-conducing SOFCs. However, due to the terrible sintering activity, fabrication of fully dense

Dr. W. P. Sun, Z. Shi, Prof. W. Liu
CAS Key Laboratory of Materials for Energy
Conversion & Collaborative Innovation Center of
Suzhou Nano Science and Technology
University of Science and Technology of China (USTC)
Hefei 230026, P.R. China
E-mail: wenping.sun@ntu.edu.sg; wliu@ustc.edu.cn

Dr. W. P. Sun
School of Materials Science and Engineering
Nanyang Technological University
50 Nanyang Avenue, Singapore 639798, Singapore

Prof. W. Liu
Key Laboratory of Materials Physics
Institute of Solid State Physics
Chinese Academy of Sciences
Hefei 230031, P. R. China

Dr. M. F. Liu
Center for Innovative Fuel Cell and Battery Technologies
School of Materials Science and Engineering
Georgia Institute of Technology
Atlanta, GA 30332, USA

Dr. L. Bi
Physical Sciences and Engineering Division
King Abdullah University of Science and Technology (KAUST)
Thuwal 23955–6900, Saudi Arabia

and highly conductive $BaZrO_3$-based films via cost-effective ceramic processes is still a considerable challenge. Recently, in order to accelerate the development of durable proton-conducting SOFCs, more and more research attention is focused on enhancing sintering activity and/or electrical conductivity of $BaZr_{0.8}Y_{0.2}O_{3-\delta}$ (BZY20), which is one of the most state-of-the-art chemically stable HTPCs.[2,10,38–45]

Sintering aids, such as ZnO,[4,44,46–49] NiO,[45] CuO,[50] CaO[43] and $LiNO_3$,[42] were successfully used to promote the sintering ability of $BaZrO_3$-based HTPCs. The $BaZrO_3$-based pellet samples could get dense at significantly reduced temperatures after adding sintering aids; however, there are very few reports about film preparation or application in fuel cells to date. Besides, the addition of sintering aids is detrimental to the total conductivity.[44,51] Even though some $BaZrO_3$-based HTPCs containing sintering aids were evaluated as electrolytes for fuel cells, the power performance of the corresponding fuel cells cannot meet the demands of practical applications at all. Peng et al.[47] prepared a 10-µm-thick $BaZr_{0.85}Y_{0.15}O_{3-\delta}$-based cell with ZnO as sintering aid and the cell showed a peak power density of only 25 mW cm^{-2} at 800 °C. Sun et al.[42] reported a 25-µm-thick BZY20-based cell with $LiNO_3$ as sintering aid, outputting merely 53 mW cm^{-2} at 700 °C. Apart from adding sintering aids, incorporating some tetravalent or trivalent metal elements into Zr-site also turns out to be a good approach. In fact, incorporating Ce into Zr site can promote the sintering of $BaZrO_3$. It was reported that sintering activity of $BaCeO_3$-$BaZrO_3$ solid solution increased with increasing the concentration of Ce.[33,35] However, as mentioned above, incorporation of Ce would decrease the chemical stability of $BaZrO_3$[32,33,35,36] and thus Ce is not an ideal dopant. Pr was found to be a promising dopant for enhancing the sintering activity while maintaining the excellent chemical stability of $BaZrO_3$-based HTPCs.[2,52] Fabbri et al.[2,53] recently developed $BaZr_{0.7}Pr_{0.1}Y_{0.2}O_{3-\delta}$ as a chemically stable and easily sintered HTPC, and the corresponding single cell delivered promising power performance. Some trivalent dopant cations, such as Sc,[54,55] In,[37,55–57] Ga,[56] and Nd,[40] were also studied to improve the sintering activity of $BaZrO_3$-based HTPCs. In-doping was found to be the most effective strategy. The sintered In-doped $BaZrO_3$ exhibited dramatically increased grain size compared to Y-doped $BaZrO_3$.[37,55,57] Unfortunately, the total conductivity decreased significantly when Y was fully substituted with In, which mainly resulted from the low bulk conductivity of In-doped $BaZrO_3$.[55,57,58] It has to be noted that, for $BaZrO_3$-based HTPCs, the conductivity is also heavily dependent on the grain size. Many results have already demonstrated that the increased grain size is very beneficial for lowering the grain-boundary resistance of $BaZrO_3$-based HTPCs.[2,41,54,57] As mentioned previously, sintering activity plays a vital role during fabricating dense $BaZrO_3$-based electrolyte films by the cost-effective ceramic processes. Therefore, Y and In co-doping might be a better choice to balance the sintering activity and proton conductivity of BZY20 towards preparing high quality BZY20-based electrolyte films for high performance proton-conducting SOFCs.

In this work, a novel chemically stable proton conductor $BaZr_{0.8}Y_{0.15}In_{0.05}O_{3-\delta}$ (BZYI5), which exhibits high proton conductivity as well as good sintering activity, was developed
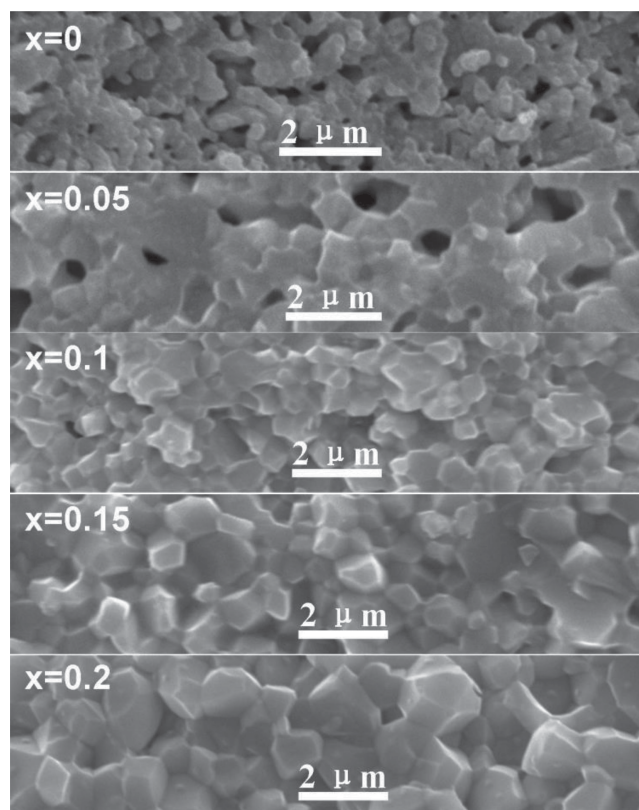

Figure 1. SEM images of the cross-sectional morphology of $BaZr_{0.8}Y_{0.2-x}In_xO_{3-\delta}$ pellets sintered at 1600 °C for 24 h in air.

by employing the strategy of Y and In co-doping. Fully dense and highly conductive BZYI5 electrolyte films were successfully prepared via a cost-effective drop-coating process. The corresponding single cells output extremely high power performance, demonstrating that desirable power densities can be attained for $BaZrO_3$-based SOFCs and BZYI5 is a promising chemically stable electrolyte material for proton-conducting SOFCs.

2. Results and Discussion

Figure 1 shows the scanning electron microscope (SEM) images of the cross-sectional morphology of the $BaZr_{0.8}Y_{0.2-x}In_xO_{3-\delta}$ pellets sintered at 1600 °C for 24 h in air. One can see that In doping promoted sintering activity of the samples substantially. The grain size of the sample grew rapidly after In incorporation and trended to grow larger with increasing In concentration. The grain size of BZY20 is around 0.5 µm, while it increases to 1 µm for $BaZr_{0.8}Y_{0.15}In_{0.05}O_{3-\delta}$ (BZYI5). Simultaneously, the relative density of the pellets increased monotonically with increasing In concentration. The relative density increased from 83.5% to 99.8% when x varied from 0 to 0.2. The sintering enhancement might be partially due to the lower melting point of In_2O_3 compared to ZrO_2 and Y_2O_3.[56,57] The difference in grain size and relative density would play an important role in the conductivity variation of the samples, and this will be discussed later.
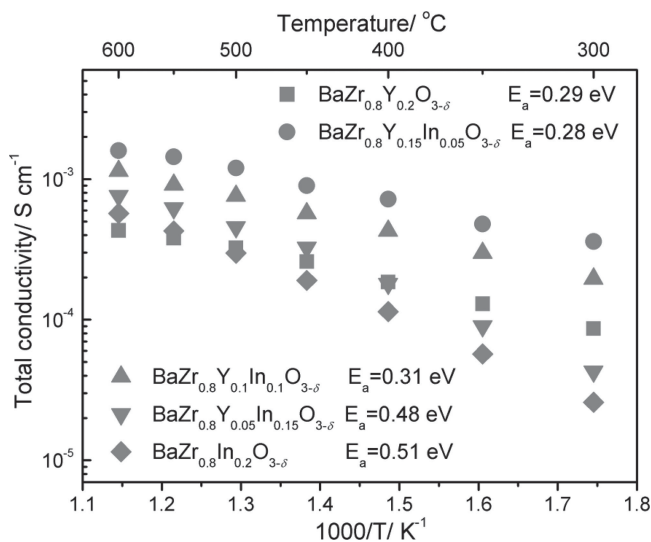
Figure 2. Arrhenius plots of the total electrical conductivity of $BaZr_{0.8}Y_{0.2-x}In_xO_{3-\delta}$ pellets measured in wet hydrogen (3% H_2O). For the sake of comparison, the conductivity of $BaZr_{0.8}In_{0.2}O_{3-\delta}$ reported in ref. [37] is shown.

In addition to sintering activity, electrical conductivity is also critical for obtaining highly conductive electrolyte films. Shown in **Figure 2** is the temperature dependence of the total electrical conductivity of $BaZr_{0.8}Y_{0.2-x}In_xO_{3-\delta}$ pellets in wet hydrogen (3% H_2O). Clearly, the conductivity was significantly dependent on the B-site doping. Among the composition series, BZYI5 exhibited the highest conductivity, which was 1.6×10^{-3} S cm^{-1} at 600 °C. For polycrystalline proton-conducting electrolytes prepared by the cost-effective ceramic process, both proton formation/transportation ability and sintering activity affect the total electrical conductivity. It can be found, for the samples modified by In, the conductivity decreased significantly with increasing In concentration, although the relatively density of the samples increased accordingly. As was reported, the formation and especially mobility of proton defects are very sensitive to the dopants for $BaZrO_3$-based oxides.[39,54,58–60] In-doped $BaZrO_3$ exhibits poorer hydration behavior and lower proton mobility than Y-doped $BaZrO_3$,[58,60] which eventually results in lower bulk conductivity of In-doped $BaZrO_3$. Moreover, as can be seen in Figure 2, the apparent activation energy (E_a) values for proton conductivity increased correspondingly with In concentration, further suggesting that protons are more easily trapped and hence more difficult to hop in crystal lattice after In-doping. On the other hand, it has to be mentioned that large grain size means low grain boundary density, which is very beneficial for decreasing grain boundary resistance of $BaZrO_3$-based oxides and attaining high total electrical conductivity.[2,41,57] Haile et al.[41] recently reported that the grain boundary conductivity of BZY20 was substantially enhanced for large-grained samples, and they found that the grain boundary conductivities differed by a factor of 2.5–3.2 for two samples with grain sizes differing by a factor of 2.3. Bi et al.[57] observed that the grain-boundary conductivity of $BaZr_{0.7}In_{0.3}O_{3-\delta}$ with larger grain size was greatly improved compared to BZY20. Accordingly, compared to BZY20, the enhanced conductivity of In-doped BZY

should be caused by the improved density and grain size of the samples. Imashuku et al.[54] found that Sc played a similar role in the co-doped compounds of $BaZr_{0.85}Sc_xY_{0.15-x}O_{3-\delta}$ (x = 0, 0.05, 0.075, 0.10, 0.15), and $BaZr_{0.85}Sc_{0.05}Y_{0.1}O_{3-\delta}$ displayed the highest total conductivity. Ito et al.[56] investigated $BaZr_{0.9}Y_{0.1-x}In_xO_{3-\delta}$ (x = 0, 0.05, 0.1), but they reported that the total conductivity decreased after introducing In. The different effect of In or Sc co-doping on the conductivity might be related with the Y concentration in the oxides, and further research is necessary to clarify this difference. It is believed that there might be a trade-off relation between the bulk and grain-boundary conductivity based on the ratio of Y and the second dopant.[54] Anyway, the present results demonstrate that Y and In co-doping is an effective approach to explore BZY20-based proton conductors showing enhanced sintering activity as well as high total electrical conductivity.

The ohmic resistance of fuel cells mainly comes from the electrolyte resistance, which is determined by the conductivity and thickness of the electrolyte materials. Thus, BZYI5, which shows the highest conductivity with improved sintering activity, is further studied and evaluated as the electrolyte materials for proton-conducting SOFCs. **Figure 3**(a) shows the X-ray diffraction (XRD) pattern of the BZYI5 powders calcined at 1100 °C for 6 h in air. Indexing of the XRD pattern clearly suggests that BZYI5 has a cubic symmetry of space group Pm-3m, which is the same as BZY20, and the corresponding lattice parameter (a) was calculated to be 4.1921 Å. High resolution transmission electron microscopy (HRTEM) (Figure 3(b)) in conjunction with selected area electron diffraction (SAED) (Figure 3(c)) further confirms that BZYI5 possesses a cubic perovskite structure. Shown in **Figure 4** is the surface chemical state of the
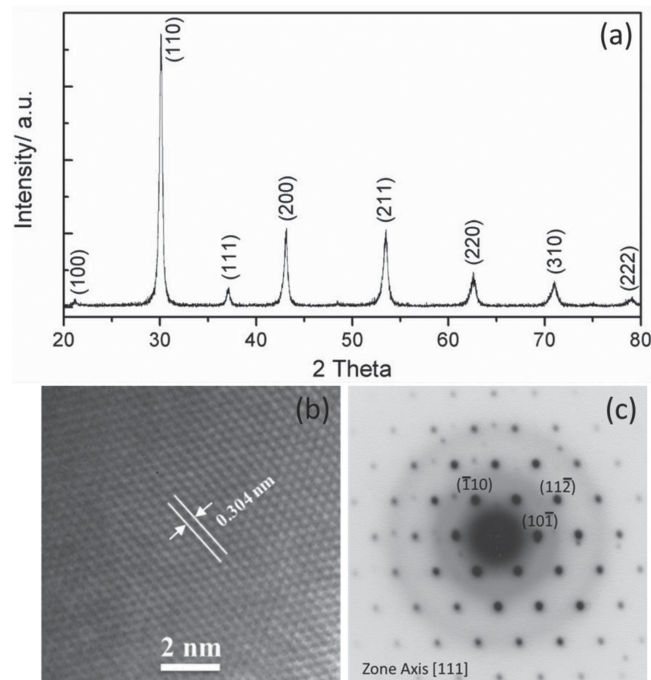
Figure 3. The XRD pattern of the BZYI5 powders calcined at 1100 °C for 6 h in air (a), the HRTEM analysis of the BZYI5 particle (b), and the corresponding SAED pattern (c).
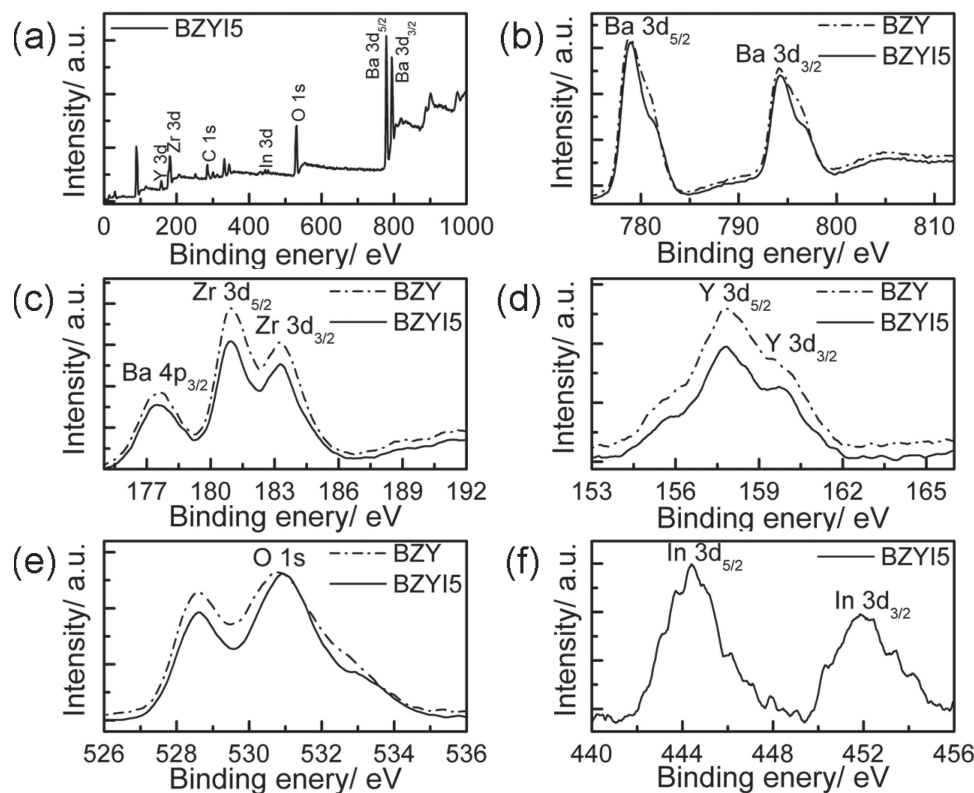
Figure 4. XPS spectra of BZYI5 and BZY20 samples: (a) survey, (b) Ba 3d, (c) Zr 3d and Ba 4p, (d) Y 3d, (e) O 1s, (f) In 3d.
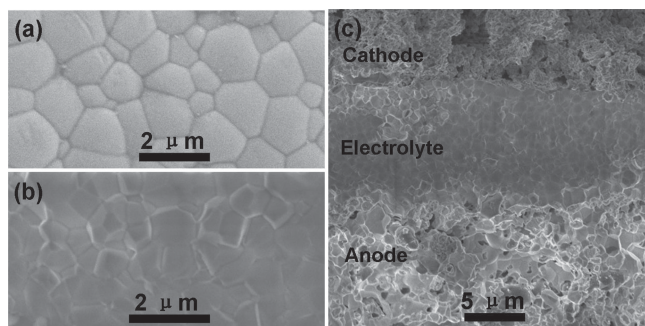
BZYI5 powders analyzed by X-ray photoelectron spectroscopy (XPS). For comparison, the XPS spectra of BZY20 are also present. Core levels of Ba $3d_{5/2}$, Ba $3d_{3/2}$, Zr 3d, Y 3d, In 3d, and O 1s can be identified in the survey spectroscopy (Figure 4(a)). The high-resolution spectra of Ba $3d_{5/2}$, Ba $4p_3$, Zr $3d_{5/2}$, Zr $3d_{3/2}$, Y $3d_{5/2}$, Y $3d_{3/2}$, O 1s, In $3d_{5/2}$, and In $3d_{3/2}$ peaks for BZY20 and BZYI5 are presented in Figure 4(b)–(f). As can be seen, the binding energy (BE) values of Ba $3d_{5/2}$, Ba $3d_{3/2}$, Ba $4p_3$, Zr $3d_{5/2}$, Zr $3d_{3/2}$, Y $3d_{5/2}$, and Y $3d_{3/2}$ core levels of BZYI5 keep the same as those of BZY20, suggesting that the crystal structure is unchanged after In doping. Notably, the O 1s peak of BZYI5 shifts slightly to the higher binding energy region compared to BZY20 (Figure 4(e)). As reported, the BE value of O 1s decreases with increasing basicity of the oxides,[38,61–63] and high basicity usually favors proton formation.[38,64,65] Thus, the hydration ability would be weakened a bit after In-doping, which is just discussed above and is in consistent with the reported results on proton formation in $BaZrO_3$-based proton conductors. Considering sintering activity plays a vital role during fabricating highly conductive polycrystalline electrolyte films by the cost-effective ceramic processes (e.g. drop coating and tape casting), to some extent, it is worth enhancing the sintering activity of the electrolytes at the expense of hydration ability and proton transport.

Indium is also an efficient dopant for increasing the chemical stability of $BaCeO_3$-based proton conductors.[29,30] As can be seen from **Figure 5**, BZYI5 still remains high chemical stability against CO_2 and water vapor after In doping. No new phases were formed after corrosive treatment in wet CO_2. In

contrast, the $BaCeO_3$-based HTPCs cannot resist the corrosion of concentrated CO_2 and water vapor at all, and some even decompose easily in 3% CO_2.[2,21,31,32] Moreover, BZYI5 also keeps excellent structural stability in H_2. Proton conductors are directly exposed in atmospheres containing H_2, water vapor or CO_2 when they are employed as electrolyte materials for SOFCs and proton-conducting phases for hydrogen separation
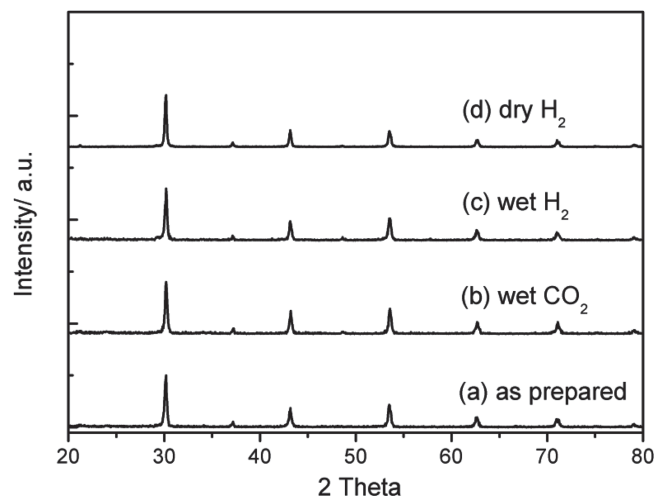
Figure 5. XRD patterns of BZYI5 powders before (a) and after exposure to wet CO_2 (3% H_2O) at 700 °C for 6 h (b), wet H_2 (3% H_2O) (c) and dry H_2 (d) at 700 °C for 12 h.

Materials
Views
www.MaterialsViews.com

ADVANCED
FUNCTIONAL
MATERIALS
www.afm-journal.de

FULL PAPER

Figure 6. SEM images of the surface morphology of the as-sintered BZYI5 electrolyte film (a), the cross-sectional morphology of the BZYI5 film (b) and single cell (c) after testing.

membranes. Thus, the high CO_2-stable and reduction-tolerant ability of BZYI5 would assure long-term operating durability for such electrochemical devices.

Due to the poor sintering activity, fabrication of high-quality BaZrO$_3$-based electrolyte films via conventional ceramic processes for proton-conducting SOFCs is still a considerable challenge. In this work, we successfully deposited fully dense BZYI5 electrolyte films on NiO-BZYI5 substrates by a drop-coating technique followed by co-firing at 1400 °C for 5 h in air. As can be seen from **Figure 6**(a) and (b), the BZYI5 film is fully dense and the grain size is in micron-scale and about 1–2 μm. No pores can be found in the film, even from the cross-sectional view of the film (Figure 6(b)). In-doping contributes significantly to obtain such dense electrolyte films. The shrinkage of the porous anode substrate during sintering would promote the densification of the electrolyte film, thereby resulting in the remarkably reduced densification temperature of the BZYI5 film compared to that of the BZYI5 pellet (as high as 1600 °C). Besides, drop coating is a promising approach for fabricating high-quality dense electrolyte films at reduced temperatures.[14,28,38,66,67] The large-grained dense electrolyte film is the fundamental for preparing single cells exhibiting low ohmic resistance and thereby outputting excellent power performance.
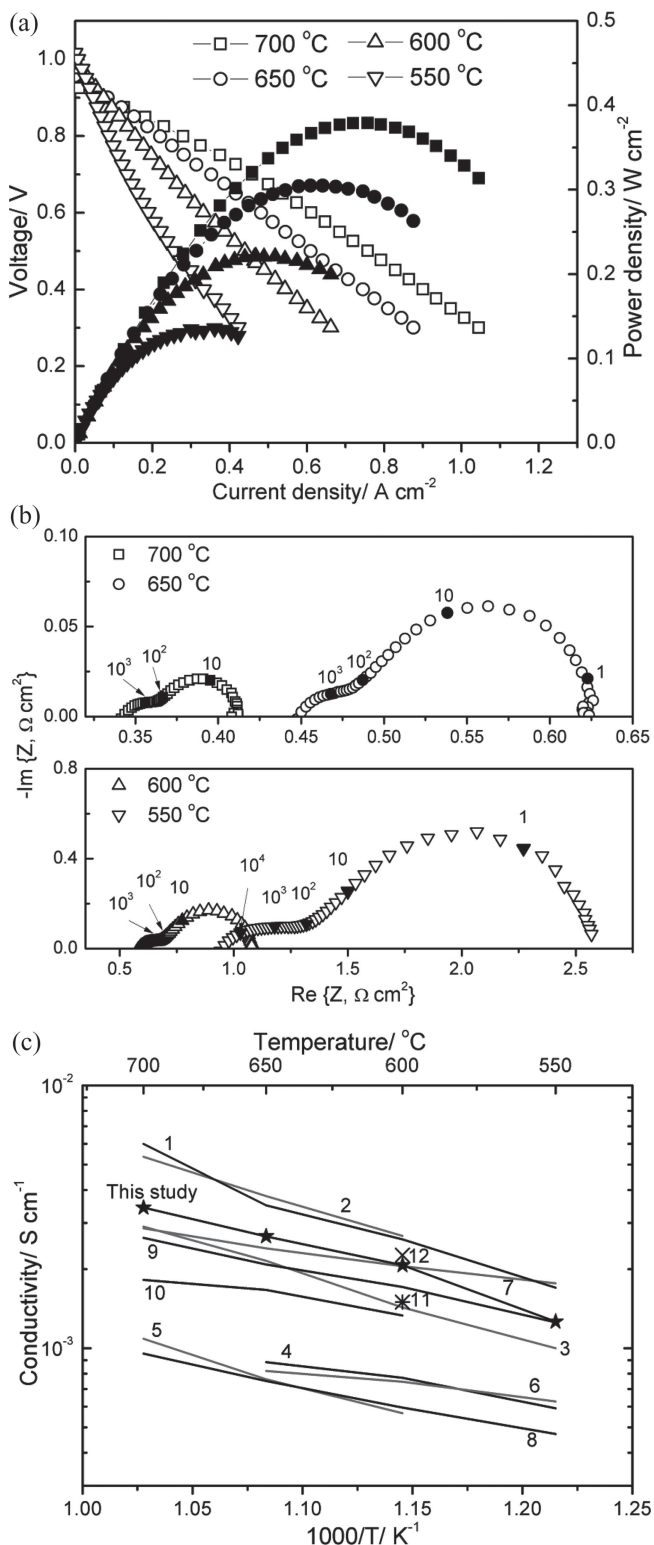
A single cell with a 12-μm-thick BZYI5 film (Figure 6(c)) and SSC–SDC cathode was tested with wet hydrogen (3% H_2O) and static air as the fuel and the oxidant, respectively. The OCV of the cell reached 0.93 0.96, 0.99, and 1.02 V at 700, 650, 600, and 550 °C, respectively, which are comparable with the reported values of BZY20-based single cells, as shown in **Table 1**. The high OCV values confirmed that the BZYI5 electrolyte film was indeed dense enough to block gas leakage and In-doping didn't introduce additional electronic conduction into the electrolyte. The I–V and power density curves of the BZYI5-based fuel cell are presented in **Figure 7**(a). The peak power densities of the single cell achieved up to 379, 306, 221, and 135 mW cm^{-2} at 700, 650, 600, and 550 °C, respectively. Obviously, the single cell performance is very encouraging and significantly enhanced compared to other fuel cells with the state-of-the-art BZY20 electrolyte films (Table 1). Compared to the ever-reported best performance of fuel cells with BZY20 electrolytes, which is 172 and 110 mW cm^{-2} at 700 and 600 °C, respectively,[68,69] the peak power density of this cell increases by 120% and 101%. The BZYI5-based fuel cell delivers much higher power performance than those anode-supported fuel cells with other sintering-improved BaZrO$_3$-based electrolytes. Sun et al.[42,43] tried LiNO$_3$ and CaO as sintering aids for BZY20, and the corresponding cells with 25-μm-thick electrolyte films output peak power density of 53 and 141 mW cm^{-2} at 700 °C, respectively. The peak power density of a cell with a 20-μm-thick BaZr$_{0.8}$Y$_{0.16}$Zn$_{0.04}$O$_{3-\delta}$ film was about 75 mW cm^{-2} at 600 °C as reported by Luisetto et al.[70] For the sinteractive BaZr$_{0.7}$Pr$_{0.1}$Y$_{0.2}$O$_{3-\delta}$ electrolyte, the corresponding cell with a 20-μm-thick electrolyte film showed peak power density of 81 mW cm^{-2} at 600 °C.[2] Even for the cell with a thinner electrolyte film (around 12 μm in thickness) and carefully engineered electrodes, the power performance was still only 163 mW cm^{-2} at 600 °C.[53] Recently, Liu and Shao et al.[40] proposed Nd-doping to enhance the sintering ability of BZY20, and the cell with a 30-μm-thick BaZr$_{0.7}$Nd$_{0.1}$Y$_{0.2}$O$_{3-\delta}$ film output power performance of 142 mW cm^{-2} at 700 °C. It should also be noted that the performance of this BZYI5-based fuel cell is comparable with and even better than many BaCeO$_3$-based proton-conducting SOFCs,[1,21,71–74] showing a great potential working at low temperatures. The present result is a substantial progress for proton-conducting SOFCs and also demonstrates that BZYI5 is a promising chemically stable electrolyte material for high performance proton-conducting SOFCs.

Table 1. Summary of the peak power density (PPD, mW cm^{-2}), electrolyte film thickness (μm), ohmic (R$_{ohm}$, Ω cm^2) and polarization resistance (R$_p$, Ω cm^2), and open circuit voltage (OCV, V) of anode supported proton-conducting SOFCs with BaZr$_{0.8}$Y$_{0.2}$O$_{3-\delta}$ electrolytes reported in the literature.

Electrolyte	Film fabrication	Film thickness [μm]	Anode; Cathode	PPD	R$_{ohm}$ [Ω cm^2]	R$_p$ [Ω cm^2]	OCV [V]	Ref.
BaZr$_{0.8}$Y$_{0.15}$In$_{0.05}$O$_{3-\delta}$	Drop coating	12	Ni-BZYI5; SSC-SDC	379 (700 °C)	0.34	0.07	0.93	This work
				221 (600 °C)	0.58	0.50	0.99	
BaZr$_{0.8}$Y$_{0.2}$O$_{3-\delta}$	Dry pressing	30	Ni-BZY20; BSCF	45 (700 °C)	–	–	0.94	[35]
BaZr$_{0.8}$Y$_{0.2}$O$_{3-\delta}$	Dry pressing	20	Ni-BZCY; SSC-SDC	170 (700 °C)	0.67	0.28	0.953	[77]
BaZr$_{0.8}$Y$_{0.2}$O$_{3-\delta}$	PLD	4	Ni-BZY20;LSCF-BCYb	110 (600 °C)	1.85	0.56	0.99	[69]
BaZr$_{0.8}$Y$_{0.2}$O$_{3-\delta}$	Dry pressing	30	Ni-BZY20; LSCF-BZPY	172 (700 °C)	0.56	0.25	0.9	[68]
BaZr$_{0.8}$Y$_{0.2}$O$_{3-\delta}$	Drop coating	25	Ni-BZCY; SSC-SDC	55 (600 °C)	3.24	1.98	0.97	[78]

BaZr$_{0.8}$Y$_{0.15}$In$_{0.05}$O$_{3-\delta}$ (BZYI5), Sm$_{0.5}$Sr$_{0.5}$CoO$_{3-\delta}$ (SSC), Ce$_{0.8}$Sm$_{0.2}$O$_{2-\delta}$ (SDC), BaZr$_{0.8}$Y$_{0.2}$O$_{3-\delta}$ (BZY20), BaZr$_{0.1}$Ce$_{0.7}$Y$_{0.2}$O$_{3-\delta}$ (BZCY), Ba$_{0.5}$Sr$_{0.5}$Co$_{0.8}$Fe$_{0.2}$O$_{3-\delta}$ (BSCF), La$_{0.6}$Sr$_{0.4}$Co$_{0.2}$Fe$_{0.8}$O$_{3-\delta}$ (LSCF), BaCe$_{0.9}$Yb$_{0.1}$O$_{3-\delta}$ (BCYb), BaZr$_{0.7}$Pr$_{0.1}$Y$_{0.2}$O$_{3-\delta}$ (BZPY).

**ADVANCED
FUNCTIONAL
MATERIALS**

www.afm-journal.de

*Materials
Views*

www.MaterialsViews.com

In order to further explore the intrinsic reasons for the excellent performance of the BZYI5-based fuel cell, electrochemical impedance spectra of the cell measured under open circuit conditions, as shown in Figure 7(b), were analyzed. In the spectra, the intercept with the real axis at high frequencies represents the ohmic resistance (R_{ohm}) of the cell, which is mainly contributed by the electrolyte resistance, and the difference between the high frequency and the low frequency intercept with the real axis represents the polarization resistance (R_p) of the cell. As can be observed, both R_{ohm} and R_p increase significantly with decreasing the operating temperature. R_{ohm} is 0.34, 0.45, 0.58, and 0.95 Ω cm^2, and R_p is 0.07, 0.17, 0.50, and 1.63 Ω cm^2 at 700, 650, 600, and 550 °C, respectively. Compared to other BZY20-based fuel cells (Table 1), R_{ohm} and R_p values are dramatically reduced, thereby inducing much better power performance. The thin, highly dense, and large-grained BZYI5 film is definitely responsible for the lower R_{ohm} values. The BZYI5 film conductivity was estimated based on R_{ohm} and film thickness, assuming that R_{ohm} is totally contributed by the electrolyte film. As shown in Figure 7(c), BZYI5 film conductivity is nearly higher than all the other BaZrO$_3$-based electrolyte films that were modified with sintering aids, suggesting that proper In-doping is a very promising strategy to promote sintering as well as keep high electrical conductivity for BaZrO$_3$. In addition to the intrinsic property of the electrolyte materials, the estimated electrolyte film conductivity is also closely associated with the fabrication method, sintering, electrode materials and microstructures. Especially, the sintering ability of anode substrate plays a key role for promoting sintering of the electrolyte and eventually obtaining dense and highly conductive electrolyte film. Bi et al.[68] fabricated a highly conductive and dense BZY20 film by the dry-pressing technique with sintering active NiO–BZY20 composite anode powders prepared by a gel combustion method, whereas the BZY20 film was still porous with mechanically mixed NiO–BZY20 anode powders. Researchers from the same group also reported that BaZr$_{0.7}$Pr$_{0.1}$Y$_{0.2}$O$_{3-\delta}$ film conductivity increased from 1.5 × 10^{-3} to 2.26 × 10^{-3} S cm^{-1} after the mechanically mixed anode powders were substituted by sintering active NiO–BZY20 composite powders.[2,53] Therefore, further conductivity improvement of the BZYI5 film can be anticipated when sintering active anode powders are used or some other fabrication parameters are optimized. Notably, the present BZYI5 film fabricated by a drop-coating technique shows higher conductivity than some other BZY20 films prepared via a ceramic fabrication process, and even higher than the BZY20 film prepared by pulsed laser deposition (PLD),[69] further suggesting that drop coating is an effective approach to prepare highly conductive BaZrO$_3$-based electrolyte films. Moreover, drop coating is more economical for fabricating large-scale films compared to PLD and dry-pressing techniques in commercial applications. R_p values reflect the kinetics of charger transfer and mass diffusion in the fuel cell, which

Figure 7. (a) *I–V* and power density curves of the BZYI5-based single cell at different operating temperatures with wet hydrogen (3% H$_2$O) as the fuel and static air as the oxidant.; (b) electrochemical impedance spectra of the BZYI5-based single cell measured under open circuit conditions. The numbers are the frequencies in hertz.; (c) comparison of conductivities of BZYI5 film and other anode-supported BaZrO$_3$-based electrolyte films estimated

under fuel cell conditions: 1) BaZr$_{0.7}$Sn$_{0.1}$Y$_{0.2}$O$_{3-\delta}$;[38] 2) BaZr$_{0.8}$Y$_{0.2}$O$_{3-\delta}$;[68] 3) BaZr$_{0.8}$Y$_{0.2}$O$_{3-\delta}$;[77] 4) BaZr$_{0.8}$Y$_{0.2}$O$_{3-\delta}$;[78] 5) BaZr$_{0.8}$In$_{0.2}$O$_{3-\delta}$;[37] 6) BaZr$_{0.7}$In$_{0.3}$O$_{3-\delta}$;[57] 7) BaZr$_{0.7}$Nd$_{0.1}$Y$_{0.2}$O$_{3-\delta}$;[40] 8) BaZr$_{0.8}$Y$_{0.2}$O$_{3-\delta}$–Li;[42] 9) BaZr$_{0.8}$Y$_{0.2}$O$_{3-\delta}$–CaO;[43] 10) BaZr$_{0.8}$Y$_{0.16}$Zn$_{0.04}$O$_{3-\delta}$;[70] 11) BaZr$_{0.7}$Pr$_{0.1}$Y$_{0.2}$O$_{3-\delta}$;[2] 12) BaZr$_{0.7}$Pr$_{0.1}$Y$_{0.2}$O$_{3-\delta}$.[53]

www.MaterialsViews.com

ADVANCED
FUNCTIONAL
MATERIALS
www.afm-journal.de

FULL PAPER

is mainly determined by the electrode materials and related microstructures. SSC–SDC, which was employed as cathode for the BZYI5-based fuel cell, was proved to be a promising high-performance cathode material for proton-conducting SOFCs.[23,26,27,38,75] The drop-coating technique is also beneficial for constructing a closely contacted anode/electrolyte interface with help of capillary force during the process for fabricating electrolyte film.[14,28,66,67] Besides highly active electrode materials, well-defined electrode/electrolyte interface is also critical for facilitating electrode reactions.[66,76] Thus, the high catalytic active electrode materials and good interfacial microstructures ensure fast electrode reactions, thereby inducing low R_p values. It should also be noted that the R_p values are still higher than some BaCeO$_3$-based proton-conducting SOFCs,[22,23,26,27,76] indicating that further effort is urgent for lowering R_p values of the BZYI5-based fuel cell. In all, the present cell performance is quite encouraging for proton-conducting SOFCs with BaZrO$_3$-based electrolytes. Serious performance improvement of BZYI5-based fuel cells can be expected by fabricating BZYI5 electrolyte films with significantly improved conductivity, exploring more efficient electrode materials, and optimizing microstructures of the fuel cell.

3. Conclusion

Y and In co-doping was demonstrated to be an effective strategy for developing sintering active and chemically stable BaZrO$_3$-based proton conductors. BZYI5 was developed as a new chemically stable proton conductor with good sintering activity and sufficiently high proton conductivity. Highly conductive and dense BZYI5 electrolyte films were successfully fabricated on the anode substrates by a cost-effective drop-coating technique followed by co-firing at 1400 °C for 5 h. The fuel cell with a dense BZYI5 electrolyte film delivered by far the best power performance among BaZrO$_3$-based fuel cells and shows a great potential working at low temperatures. Additional performance improvement is possible by further improving BZYI5 film conductivity, exploring more efficient electrode materials, and optimizing microstructures of the fuel cell.

4. Experimental Section

Synthesis: BaZr$_{0.8}$Y$_{0.2-x}$In$_x$O$_{3-\delta}$ (x = 0, 0.05, 0.1, 0.15, 0.2) powders were synthesized via a typical citric acid-nitrate gel combustion process.[77] Firstly, Y$_2$O$_3$ was dissolved in diluted nitric acid under heating. Then, Zr(NO$_3$)$_4$·5H$_2$O and In(NO$_3$)$_4$·4.5H$_2$O were added with stirring and heating on a hot plate. After the solution got clear, Ba(CH$_3$COO)$_2$ was then added. Citric acid was added in metal ions: citric acid molar ratio of 1:1.5 and the pH value was adjusted to about 7 with NH$_3$·H$_2$O. The solution was heated and stirred continuously at about 70 °C until gelling. After a while, gel ignition and combustion occurred, yielding the as-prepared black powders. Finally, the black powders were calcined at 1100 °C for 6 h in air, obtaining BaZr$_{0.8}$Y$_{0.2-x}$In$_x$O$_{3-\delta}$ powders with a cubic perovskite structure (Supporting Information, Figure S1). The BaZr$_{0.8}$Y$_{0.2-x}$In$_x$O$_{3-\delta}$ pellets were sintered at 1600 °C for 24 h in static air, and all the pellets still kept cubic perovskite structures after sintering (Supporting Information, Figure S2).

Characterization and Electrochemical Measurements: Phase structures of the powders and pellets were identified by an X-ray diffractometer (Rigaku TTR-?) using CuKα radiation. High resolution transmission electron microscope (HRTEM) of BaZr$_{0.8}$Y$_{0.15}$In$_{0.05}$O$_{3-\delta}$ (BZYI5) particles was taken from JEM-2010. The XPS spectra of the powders were collected using an X-ray photoelectron spectrometer (ESCALAB250, Thermo-VG Scientific, UK) using monochromatized Al Kα radiation (1486.92 eV). Measurements were performed in a Constant Analyzer Energy (CAE) mode with 70 eV pass energy for survey spectra and 20 eV for high resolution spectra. The relative density of the sintered pellets was measured via a typical Archimedes method. The microstructure of the sintered pellets was examined by scanning electron microscope (SEM, JEOL JSM-6700F). The total electrical conductivity of the sintered pellets in wet hydrogen (3% H$_2$O) was studied via a two-point method using an impedance analyzer (CHI604B, Chenhua Inc., Shanghai) with an amplitude of 5 mV in the frequency range from 100 kHz to 0.1 Hz. Pt paste was brush-painted symmetrically on both sides of the sintered pellets as current collectors and then fired at 950 °C for 1 h to remove the residual organics and attain good adhesion between the pellet and Pt layer. The BZYI5 electrolyte films were fabricated by a drop-coating process on the NiO–BZYI5 (65:35, weight ratio) anode substrates followed by co-firing at 1400 °C for 5 h in air.[28,66] The BZYI5 powders were firstly dispersed in ethanol with polyvinyl butyral (PVB, binder, 4%) and triethanolamine (TEA, dispersant, 6%), and were then ball milled for 48 h to obtain a BZYI5 electrolyte suspension. The BZYI5 suspension was deposited onto the NiO–BZYI5 anode substrate by a transferpettor. The electrolyte film thickness can be controlled by varying the suspension volume during coating. For full cell preparation, Sm$_{0.5}$Sr$_{0.5}$CoO$_{3-\delta}$–Ce$_{0.8}$Sm$_{0.2}$O$_{2-\delta}$ (SSC–SDC, 3:2, weight ratio) composite cathode slurry was brush-painted onto the BZYI5 electrolyte film followed by firing at 950 °C for 2 h in air to form a porous cathode layer with an effective cathode area of 0.3 cm^2. Silver wire and silver paste was used for current collection. For fuel cell performance measurement, the single cell was sealed onto an alumina fuel cell testing fixture with ceramic paste (Ceramabond 552, Aremco). Wet hydrogen (3% H$_2$O) and static air was used as the fuel and the oxidant, respectively. The single cell was tested using an Arbin multichannel electrochemical testing system (MSTAT). The flow rate of the fuel gas was about 30 mL min^{-1}. Electrochemical impedance spectra of the cell were performed using a Solartron 1255 HF frequency response analyzer, interfaced with an EG&G PAR potentiostat model 273A with an amplitude of 10 mV in the frequency range from 100 kHz to 0.1 Hz. The microstructure of the BZYI5 film and tested cell was examined by scanning electron microscope (SEM, LEO 1530).

Supporting Information

Supporting Information is available from the Wiley Online Library or from the author.

Acknowledgements

[1] C. Zuo, S. Zha, M. Liu, M. Hatano, M. Uchiyama, *Adv. Mater.* **2006**, *18*, 3318.
[2] E. Fabbri, L. Bi, H. Tanaka, D. Pergolesi, E. Traversa, *Adv. Funct. Mater.* **2011**, *21*, 158.

[3] E. Fabbri, D. Pergolesi, E. Traversa, *Chem. Soc. Rev.* **2010**, *39*, 4355.

[4] S. W. Tao, J. T. S. Irvine, *Adv. Mater.* **2006**, *18*, 1581.

[5] B. C. Steele, A. Heinzel, *Nature* **2001**, *414*, 345.

[6] E. D. Wachsman, K. T. Lee, *Science* **2011**, *334*, 935.

[7] H. Iwahara, T. Esaka, H. Uchida, N. Maeda, *Solid State Ionics* **1981**, *3–4*, 359.

[8] K. D. Kreuer, *Annu. Rev. Mater. Res.* **2003**, *33*, 333.

[9] R. Haugsrud, T. Norby, *Nat. Mater.* **2006**, *5*, 193.

[10] D. Pergolesi, E. Fabbri, A. D'Epifanio, E. Di Bartolomeo, A. Tebano, S. Sanna, S. Licoccia, G. Balestrino, E. Traversa, *Nat. Mater.* **2010**, *9*, 846.

[11] L. Yang, S. Z. Wang, K. Blinn, M. F. Liu, Z. Liu, Z. Cheng, M. L. Liu, *Science* **2009**, *326*, 126.

[12] S. Fang, L. Bi, X. Wu, H. Gao, C. Chen, W. Liu, *J. Power Sources* **2008**, *183*, 126.

[13] C. D. Zuo, S. E. Dorris, U. Balachandran, M. L. Liu, *Chem. Mater.* **2006**, *18*, 4647.

[14] M. Liu, W. Sun, X. Li, S. Feng, D. Ding, D. Chen, M. Liu, H. C. Park, *Int. J. Hydrogen Energ.* **2013**, *38*, 14743.

[15] S. Fang, K. S. Brinkman, F. Chen, *J. Membrane Sci.* **2014**, *467*, 85.

[16] S. Fang, K. Brinkman, F. Chen, *ACS Appl. Mater. Interfaces* **2014**, *6*, 725.

[17] S. Fang, S. Wang, K. S. Brinkman, F. Chen, *J. Mater. Chem. A* **2014**, *2*, 5825.

[18] F. He, D. Song, R. Peng, G. Meng, S. Yang, *J. Power Sources* **2010**, *195*, 3359.

[19] Y. Y. Rao, Z. Q. Wang, W. Zhong, R. R. Peng, Y. L. Lu, *J. Power Sources* **2012**, *199*, 142.

[20] R. R. Peng, Y. Wu, L. Z. Yang, Z. Q. Mao, *Solid State Ionics* **2006**, *177*, 389.

[21] L. Bi, S. Q. Zhang, S. M. Fang, Z. T. Tao, R. R. Peng, W. Liu, *Electrochem. Commun.* **2008**, *10*, 1598.

[22] L. Yang, C. Zuo, S. Wang, Z. Cheng, M. Liu, *Adv. Mater.* **2008**, *20*, 3280.

[23] W. P. Sun, L. T. Yan, B. Lin, S. Q. Zhang, W. Liu, *J. Power Sources* **2010**, *195*, 3155.

[24] W. P. Sun, S. M. Fang, L. T. Yan, W. Liu, *J. Electrochem. Soc.* **2011**, *158*, B1432.

[25] B. H. Rainwater, M. F. Liu, M. L. Liu, *Int. J. Hydrogen Energ.* **2012**, *37*, 18342.

[26] Z. Shi, W. Sun, W. Liu, *J. Power Sources* **2014**, *245*, 953.

[27] Z. Shi, W. Sun, Z. Wang, J. Qian, W. Liu, *ACS Appl. Mater. Interfaces* **2014**, *6*, 5175.

[28] M. F. Liu, J. F. Gao, X. Q. Liu, G. Y. Meng, *Int. J. Hydrogen Energ.* **2011**, *36*, 13741.

[29] F. Zhao, Q. Liu, S. Wang, K. Brinkman, F. Chen, *Int. J. Hydrogen Energ.* **2010**, *35*, 4258.

[30] L. Bi, S. Zhang, L. Zhang, Z. Tao, H. Wang, W. Liu, *Int. J. Hydrogen Energ.* **2009**, *34*, 2421.

[31] F. L. Chen, O. T. Sorensen, G. Y. Meng, D. K. Peng, *J. Mater. Chem.* **1997**, *7*, 481.

[32] C. S. Tu, R. R. Chien, V. H. Schmidt, S. C. Lee, C. C. Huang, C. L. Tsai, *J. Appl. Phy.s* **2009**, *105*, 103504.

[33] E. Fabbri, A. Depifanio, E. Dibartolomeo, S. Licoccia, E. Traversa, *Solid State Ionics* **2008**, *179*, 558.

[34] K. H. Ryu, S. M. Haile, *Solid State Ionics* **1999**, *125*, 355.

[35] Y. Guo, Y. Lin, R. Ran, Z. Shao, *J. Power Sources* **2009**, *193*, 400.

[36] S. Ricote, N. Bonanos, G. Caboche, *Solid State Ionics* **2009**, *180*, 990.

[37] W. Sun, Z. Zhu, Z. Shi, W. Liu, *J. Power Sources* **2013**, *229*, 95.

[38] W. P. Sun, M. F. Liu, W. Liu, *Adv. Energy. Mater.* **2013**, *3*, 1041.

[39] Y. Yamazaki, F. Blanc, Y. Okuyama, L. Buannic, J. C. Lucio-Vega, C. P. Grey, S. M. Haile, *Nat. Mater.* **2013**, *12*, 647.

[40] Y. Liu, Y. Guo, R. Ran, Z. Shao, *J. Membrane Sci.* **2012**, *415–416*, 391.

[41] Y. Yamazaki, R. Hernandez-Sanchez, S. M. Haile, *Chem. Mater.* **2009**, *21*, 2755.

[42] Z. Sun, E. Fabbri, L. Bi, E. Traversa, *Phys. Chem. Chem. Phys.* **2011**, *13*, 7692.

[43] Z. Sun, E. Fabbri, L. Bi, E. Traversa, *J. Am. Ceram. Soc.* **2012**, *95*, 627.

[44] C. Peng, J. Melnik, J.-L. Luo, A. R. Sanger, K. T. Chuang, *Solid State Ionics* **2010**, *181*, 1372.

[45] J. Tong, D. Clark, M. Hoban, R. O'Hayre, *Solid State Ionics* **2010**, *181*, 496.

[46] P. Babilo, S. M. Haile, *J. Am. Ceram. Soc.* **2005**, *88*, 2362.

[47] C. Peng, J. Melnik, J. Li, J. Luo, A. R. Sanger, K. T. Chuang, *J. Power Sources* **2009**, *190*, 447.

[48] S. Tao, J. T. S. Irvine, *J. Solid State Chem.* **2007**, *180*, 3493.

[49] X. Xu, S. Tao, J. T. S. Irvine, *J. Solid State Chem.* **2010**, *183*, 93.

[50] D. Gao, R. Guo, *J. Alloy Compd* **2010**, *493*, 288.

[51] M. Amsif, D. Marrero-Lopez, J. C. Ruiz-Morales, S. N. Savvin, P. Nunez, *J. Power Sources* **2011**, *196*, 9154.

[52] A. Magrasó, C. Frontera, A. E. Gunnæs, A. Tarancón, D. Marrero-López, T. Norby, R. Haugsrud, *J. Power Sources* **2011**, *196*, 9141.

[53] E. Fabbri, L. Bi, J. M. Rupp, D. Pergolesi, E. Traversa, *RSC Adv.* **2011**, *1*, 1183.

[54] S. Imashuku, T. Uda, Y. Nose, K. Kishida, S. Harada, H. Inui, Y. Awakura, *J. Electrochem. Soc.* **2008**, *155*, B581.

[55] S. Imashuku, T. Uda, Y. Nose, G. Taniguchi, Y. Ito, Y. Awakura, *J. Electrochem. Soc.* **2009**, *156*, B1.

[56] N. Ito, H. Matsumoto, Y. Kawasaki, S. Okada, T. Ishihara, *Solid State Ionics* **2008**, *179*, 324.

[57] L. Bi, E. Fabbri, Z. Sun, E. Traversa, *Solid State Ionics* **2011**, *196*, 59.

[58] K. D. Kreuer, S. Adams, W. Munch, A. Fuchs, U. Klock, J. Maier, *Solid State Ionics* **2001**, *145*, 295.

[59] D. L. Han, Y. Nose, K. Shinoda, T. Uda, *Solid State Ionics* **2012**, *213*, 2.

[60] D. Zeudmi Sahraoui, T. Mineva, *Solid State Ionics* **2013**, *253*, 195.

[61] V. Dimitrov, T. Komatsu, R. Sato, *J. Ceram. Soc. Jpn* **1999**, *107*, 21.

[62] T. Honma, R. Sato, Y. Benino, T. Komatsu, V. Dimitrov, *J. Non-Cryst. Solids* **2000**, *272*, 1.

[63] Q. Zeng, Y. B. Zu, C. G. Fan, C. S. Chen, *J. Membrane Sci.* **2009**, *335*, 140.

[64] K. D. Kreuer, *Solid State Ionics* **1997**, *97*, 1.

[65] K. D. Kreuer, *Solid State Ionics* **1999**, *125*, 285.

[66] M. Liu, D. Dong, R. Peng, J. Gao, J. Diwu, X. Liu, G. Meng, *J. Power Sources* **2008**, *180*, 215.

[67] M. Liu, J. Gao, D. Dong, X. Liu, G. Meng, *Int. J. Hydrogen Energ.* **2010**, *35*, 10489.

[68] L. Bi, E. Fabbri, Z. Sun, E. Traversa, *Energ. Environ. Sci.* **2011**, *4*, 1352.

[69] D. Pergolesi, E. Fabbri, E. Traversa, *Electrochem. Commun.* **2010**, *12*, 977.

[70] I. Luisetto, S. Licoccia, A. D'Epifanio, A. Sanson, E. Mercadelli, E. Di Bartolomeo, *J. Power Sources* **2012**, *220*, 280.

[71] Z. W. Zhu, Z. T. Tao, L. Bi, W. Liu, *Mater. Res. Bull.* **2010**, *45*, 1771.

[72] B. Lin, H. P. Ding, Y. C. Dong, S. L. Wang, X. Z. Zhang, D. Fang, G. Y. Meng, *J. Power Sources* **2009**, *186*, 58.

[73] Z. T. Tao, L. Bi, L. T. Yan, W. P. Sun, Z. W. Zhu, R. R. Peng, W. Liu, *Electrochem. Commun.* **2009**, *11*, 688.

[74] F. Zhao, F. L. Chen, *Int. J. Hydrogen Energ.* **2010**, *35*, 11194.

[75] L. Zhao, B. He, J. Gu, F. Liu, X. Chu, C. Xia, *Int. J. Hydrogen Energ.* **2012**, *37*, 548.

[76] W. P. Sun, Z. W. Zhu, Y. Z. Jiang, Z. Shi, L. T. Yan, W. Liu, *Int. J. Hydrogen Energ.* **2011**, *36*, 9956.

[77] W. P. Sun, L. T. Yan, Z. Shi, Z. W. Zhu, W. Liu, *J. Power Sources* **2010**, *195*, 4727.

[78] J. Xiao, W. P. Sun, Z. W. Zhu, Z. T. Tao, W. Liu, *Mater. Lett.* **2012**, *73*, 198.